Gain Scheduling Control of Control Moment Gyroscope

M2015SC007 Toru INABA

Supervisor: Isao TAKAMI

Abstract

This paper presents gain scheduling (GS) control of a Variable Speed Control Moment Gyroscope (VSCMG) based on sum of squares (SOS). Nonlinear motion equations of the VSCMG are complicated because they contain sine and cosine of angles of gimbals. The dynamics varies depending on an attitude of a spacecraft. In this study, the difficulty of control design of the VSCMG is solved by two methods. First, the complex nonlinear model is transformed to the linear parameter varying (LPV) model, which the linear control method can be applied, to make prospect of control design easy by using a proposed approximation method. The highly accurate LPV model is reduced to polynomially parameter-dependent linear matrix inequalities (PDLMIs). Second, GS controller whose gains are adjusted depending on the angles and the attitude is applied. The polynomially PDLMIs can be relaxed to finite design conditions based on matrix SOS polynomials. The GS controller is designed by solving the finite SOS conditions. By using those methods, GS controller which appropriately calculates gains depending on the nonlinearities is designed. The effectiveness of the proposed controller is illustrated by simulations and experiments.

1 Introduction

A Control Moment Gyroscope (CMG) is known as an attitude control device for space crafts. The CMG is an attractive actuator because the maximum torque generated by a CMG is dozens of times compared with the torque by a conventional actuator called reaction wheel. In this study, the control design of a single-Variable Speed CMG (VSCMG) is treated as a fundamental study for cooperation control of CMGs. The VSCMG consists of a variable speed reaction wheel and a single gimbal. It is not easy to adopt general linear control methods to the VSCMG, because the dynamics of the VSCMG varies depending on an attitude of the spacecraft. Nonlinear control methods are adopted to the controller design of the VSCMG. Recently, gridding-based gain scheduling (GS) controller design based on a linear parameter varying (LPV) system is reported to solve the nonlinear dynamics [1], while robust stability of the system is guaranteed by solving many linear matrix inequalities (LMIs).

This paper presents a GS controller design of the VSCMG based on sum of squares (SOS). The VSCMG which has the multi-freedom actuator is able to control two-degrees-of-freedom (DOF) attitude, but the controller design is very complicated to include many nonlinearities such as sine and cosine of the gimbal's angles in the motion equations. Let $\theta(t)$ be a time varying parameter in the motion equations. Nonlinearities such as $\sin\theta(t)$ and $\cos\theta(t)$ in motion equations are generally approximated by the first-order Taylor series expansion to get a simplified linear model. The nonlinearity $\sin\theta(t)$ is assumed to be a varying parameter and an approximation depending on $\sin\theta(t)$ is applied only to $\cos\theta(t)$ in our study. In this study, in order to conduct a highly accurate approximation, the third-order Padé

approximation is applied. A highly accurate LPV model including rational function of the varying parameter is derived by the proposed approximation method. In this study, the GS controller is designed to adjust gains depending on the nonlinear dynamics of the VSCMG. The GS controller is designed based on matrix SOS polynomials, because the polynomially parameter-dependent linear matrix inequalities (PDLMIs) are relaxed to finite matrix SOS polynomials conditions, naturally. The conservativeness of the GS controller designed by the proposed approximation method is lower comparing with a GS controller designed by an ordinary approximation method. The effectiveness of our proposed GS controller is shown by simulations and experiments comparing with an ordinary GS controller.

2 Attitude Control Model of a VSCMG

2.1 Hardware and System Restriction

Model 750 CMG having the variable speed wheel is 4-DOF control plant. The schematic diagram of Model 750 CMG is shown in Fig. 1. It consists of four rigid
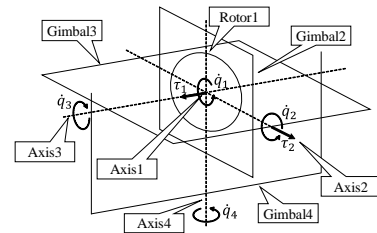
Figure 1 Model 750 Control Moment Gyroscope

bodies which are Rotor1, Gimbal2, Gimbal3, and Gimbal4. Rotor1 and Gimbal2 are a VSCMG. Gimbal3 and Gimbal4 are controlled bodies. These bodies rotate around Axis1, 2, 3, and 4. Here, let q_1, q_2, q_3, and q_4 be the angles of Rotor1, Gimbal2, Gimbal3, and Gimbal4, respectively. And, $\dot{q}_1, \dot{q}_2, \dot{q}_3$, and $\dot{q}_4$ indicate the angular velocity of Rotor1, Gimbal2, Gimbal3, and Gimbal4, respectively. Let τ_1 and τ_2 be the input torque for Rotor1 and Gimbal2, respectively. Note that the VSCMG which is used in this study has a hardware restriction on the motion range of Gimbal2. The motion range of Gimbal2 is $\pm\pi/2$[rad] from the vertical position to Gimbal3. Rotor1 and Gimbal2 are driven by DC motors, while Gimbal3 and Gimbal4 have no drive source. Gimbal3 and Gimbal4 are driven by reaction torque and gyroscopic precession, respectively. These torque are generated by the VSCMG. The gyroscopic precession is largest when the position of Gimbal2 is tilted rapidly around the vertical position to Gimbal3. The motion range of Gimbal2 is assumed as follows:

$$-\frac{\pi}{6} \leq q_2 \leq \frac{\pi}{6}. \tag{1}$$

An attitude of Gimbal3 is given by the angles q_3 and q_4. The attitude is regarded as an attitude of a spacecraft. The motion range of Gimbal3 is restricted, because the system has singular points depending on the attitude

of Gimbal3. The singular points are the positions of $\pm\pi/2$[rad] from the vertical position to Gimbal4. The motion range of Gimbal3 is assumed as follows:

$$-\frac{5\pi}{12} \le q_3 \le \frac{5\pi}{12}. \tag{2}$$

In this study, MIMO system which ensure the stability of the responses q_3 and q_4 under the motion range (1) and (2) is treated.

2.2 Nonlinear Model

In this subsection, motion equations of Model 750 CMG are derived. If the angular velocity $\dot{q}_1$ is large enough compared with other angular velocity $\dot{q}_2$, $\dot{q}_3$, and $\dot{q}_4$, a simplified nonlinear mathematical model is derived [1]. Thus, motion equations of Model 750 CMG is represented as follows:

$$
\begin{bmatrix}
b_3 & 0 \\
0 & b_{12}\sin^2 q_2 - b_1 + b_4 \\
-b_3\sin q_3 & -b_{12}\sin q_2\cos q_2\cos q_3
\end{bmatrix}
$$
$$
\begin{bmatrix}
-b_3\sin q_3 \\
-b_{12}\sin q_2\cos q_2\cos q_3 \\
-b_{12}\sin^2 q_2(1-\sin^2 q_3) + b_5\sin^2 q_3 + b_6
\end{bmatrix}
\begin{bmatrix}
\ddot{q}_2 \\
\ddot{q}_3 \\
\ddot{q}_4
\end{bmatrix}
$$
$$
+\begin{bmatrix}
0 & \dot{q}_1 b_1\sin q_2 \\
-\dot{q}_1 b_1\sin q_2 & 0 \\
\dot{q}_1 b_1\cos q_2\cos q_3 & -\dot{q}_1 b_1\sin q_2\sin q_3
\end{bmatrix}
$$
$$
\begin{bmatrix}
-\dot{q}_1 b_1\cos q_2\cos q_3 \\
\dot{q}_1 b_1\sin q_2\sin q_3 \\
0
\end{bmatrix}
\begin{bmatrix}
\dot{q}_2 \\
\dot{q}_3 \\
\dot{q}_4
\end{bmatrix}
$$
$$
=\begin{bmatrix}
0 & 1 \\
-\cos q_2 & 0 \\
-\sin q_2\cos q_3 & 0
\end{bmatrix}
\begin{bmatrix}
\tau_1 \\
\tau_2
\end{bmatrix}, \tag{3}
$$
$$
\begin{cases}
b_{12}=b_1+b_2,\ b_1=J_D,\ b_2=I_D-J_C-J_D+K_C, \\
b_3=I_C+I_D,\ b_5=I_B+I_C-K_B-K_C, \\
b_4=J_B+J_C+J_D,\ b_6=I_D+K_A+K_B+K_C.
\end{cases}
$$

I_x, J_x, and K_x ($x = A, B, C, D$) are the moment of inertia. As can be seen in (3), there exist nonlinearities such as $\sin q_i$ and $\cos q_i$ ($i = 2, 3$).

2.3 Linear Parameter Varying (LPV) Modeling

In this subsection, our model approximation method is proposed. Assume that there exist nonlinear terms such as $\sin\theta(t)$ and $\cos\theta(t)$ in motion equations. The nonlinearity of $\sin\theta(t)$ is a varying parameter such as $\alpha(t) := \sin\theta(t)$. The other nonlinearity of $\cos\theta(t)$ is represented as $\cos\theta(t) = \sqrt{1-\alpha(t)^2}$. Approximation is done only for $\cos\theta(t)$ by using Taylor series expansion or Padé approximation depending on $\sin\theta(t)$. Thus, if the nonlinearity of the sine function in (3) are defined as $\alpha_i := \sin q_i$, the nonlinearity of cosine function are represented as $\cos q_i = \sqrt{1-\alpha_i^2}$. The square roots are approximated by using Taylor series expansion or Padé approximation under the motion range (1) and (2). The square root $\sqrt{1-\alpha_2^2}$ is approximated by second-order Taylor series expansion. The other square root $\sqrt{1-\alpha_3^2}$ is more accurately approximated by third-order Padé approximation. Those approximations are represented as follows:

$$\cos q_2 \simeq 1 - \frac{\alpha_2^2}{2}, \quad \cos q_3 \simeq \frac{1-\alpha_3^2}{1-\alpha_3^2/2}. \tag{4}$$

Furthermore, the coefficients in (4) are optimized by using the method of least-squares to conduct more accurate approximation under the range (1) and (2), respectively. Note that the approximated functions pass the upper bound value of $\cos q_i$. Consequently, our model approximation method is proposed as follows:

$$\begin{cases} \sin q_2 = \alpha_2 \\ \cos q_2 \simeq 1 - 0.5251\alpha_2^2 =: \alpha_p \end{cases}, \tag{5}$$

$$\begin{cases} \sin q_3 = \alpha_3 \\ \cos q_3 \simeq \dfrac{1-0.8943\alpha_3^2}{1-0.4401\alpha_3^2} =: \alpha_r \end{cases}. \tag{6}$$

The true values of the square root and its approximated values of α_p and α_r are illustrated in Fig. 2. The dot-
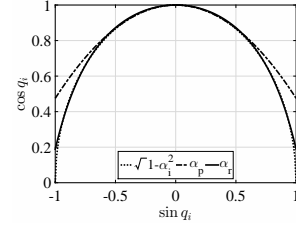
Figure 2 Approximation

ted curve, long dashed short dashed curve, and the solid curve show the true values of the square root and the approximated value a_p, and the approximated value a_r respectively. The maximum relative error between the true value and the approximated value of α_p and α_r is 0.31% and 8.55% in the range (1) and (2), respectively. Here, let $\boldsymbol{x} = [\dot{q}_2\ \dot{q}_3\ \dot{q}_4]^{\mathrm{T}}$, $\boldsymbol{u} = [\tau_1\ \tau_2]^{\mathrm{T}}$, and $\boldsymbol{\alpha} = [\alpha_2\ \alpha_3]^{\mathrm{T}}$ be the state variable vector, the control input vector, and the varying parameter vector, respectively. The linear parameter varying (LPV) system is represented as follows by using the proposed method:

$$\boldsymbol{E}(\boldsymbol{\alpha})\dot{\boldsymbol{x}} = \boldsymbol{A}(\boldsymbol{\alpha})\boldsymbol{x} + \boldsymbol{B}(\boldsymbol{\alpha})\boldsymbol{u}, \tag{7}$$

There exist the rational function of the varying parameter α_3 in the matrices $\boldsymbol{E}(\boldsymbol{\alpha})$, $\boldsymbol{A}(\boldsymbol{\alpha})$, and $\boldsymbol{B}(\boldsymbol{\alpha})$ in (7). It is not easy to reduce the system (7) to parameter-dependent linear matrix inequalities (PDLMIs) for control design. Descriptor representation and linear fractional transformation (LFT) is applied to the system(7) to get a LPV model which do not include the rational function of the varying parameter α_3. The LPV model (7) is transformed to an equivalent system with fourth-order polynomials of the varying parameters α_i by using those methods. First, the redundant descriptor representation is applied. The varying parameters α_i are integrated into a new matrix $\hat{\boldsymbol{A}}$ by introducing a redundant descriptor variable vector as $\hat{\boldsymbol{x}} := [\boldsymbol{x}^{\mathrm{T}}\ \dot{\boldsymbol{x}}^{\mathrm{T}}\ \tau_1]^{\mathrm{T}}$. The redundant descriptor representation is obtained as follows:

$$\hat{\boldsymbol{E}}\dot{\hat{\boldsymbol{x}}} = \hat{\boldsymbol{A}}(\boldsymbol{\alpha})\hat{\boldsymbol{x}} + \hat{\boldsymbol{B}}(\boldsymbol{\alpha})\boldsymbol{u}, \tag{8}$$

Second, LFT is applied to the redundant descriptor system (8) including the rational function of the varying parameter α_3 to get a LPV model including fourth-order polynomials of the varying parameter α_i. Here, the matrix $\hat{\boldsymbol{A}}$ is expressed as

$$\hat{\boldsymbol{A}} = \boldsymbol{A}_n + \boldsymbol{B}_\delta(\boldsymbol{I} - \boldsymbol{\Delta}\boldsymbol{D}_\delta)^{-1}\boldsymbol{\Delta}\boldsymbol{C}_\delta. \tag{9}$$

By using the matrices $\boldsymbol{A}_n, \boldsymbol{B}_\delta, \boldsymbol{C}_\delta, \boldsymbol{D}_\delta, \boldsymbol{I}$, and $\boldsymbol{\Delta}$ satisfying the equivalent condition (9), the redundant system is rewritten as follows:

$$\hat{\boldsymbol{E}}_\delta \dot{\hat{\boldsymbol{x}}}_\delta = \hat{\boldsymbol{A}}_\delta(\boldsymbol{\alpha})\,\hat{\boldsymbol{x}}_\delta + \hat{\boldsymbol{B}}_\delta(\boldsymbol{\alpha})\,\boldsymbol{u} \qquad (10)$$

As can be seen in (10), there exist fourth-order polynomial functions of the varying parameter α_i. The LPV model that is equivalent to the system (7) is obtained.

3 Controller Synthesis

3.1 Gain Scheduling Controller Design

A gain scheduling (GS) controller is designed by choosing the scheduling parameter vector $\boldsymbol{\alpha} \in \mathbb{R}^2$. The purpose of our study is to achieve attitude control of Gimbal3 and Gimbal4. The angles q_3 and q_4 are added to the state variable vector $\boldsymbol{x}$ in (7). Let q_3^{ref} and q_4^{ref} be given constant references for the angles q_3 and q_4, respectively. The output equation is defined as follows:

$$\boldsymbol{y} = \boldsymbol{C} \boldsymbol{x}_e, \qquad (11)$$

where $\boldsymbol{y} = [q_3 \ q_4]^{\mathrm{T}}, \boldsymbol{C} = [\boldsymbol{I}_2 \ \boldsymbol{0}_{2\times5}], \boldsymbol{x}_e := [q_3 \ q_4 \ \boldsymbol{x}^{\mathrm{T}}]^{\mathrm{T}}$. To follow the reference without steady-state error, servo system is adopted as follows:

$$\boldsymbol{u} = \boldsymbol{K}(\boldsymbol{\alpha})\,\boldsymbol{x}_e + \boldsymbol{G}(\boldsymbol{\alpha}) \int_0^\infty \left(\boldsymbol{y}^{\mathrm{ref}} - \boldsymbol{y}\right) dt, \quad (12)$$

where $\boldsymbol{y}^{\mathrm{ref}} := [q_3^{\mathrm{ref}} \ q_4^{\mathrm{ref}}]^{\mathrm{T}}$. The GS controller consists of not the redundant descriptor variable vector $\hat{\boldsymbol{x}}_\delta$ but the original state variable vector $\boldsymbol{x}_e$.

In this study, linear quadratic (LQ) optimal control is adopted to evaluate a initial-value response. A cost function is introduced as follows [2]:

$$J = \int_0^\infty \left(\tilde{\boldsymbol{x}}_\delta^{\mathrm{T}} \tilde{\boldsymbol{Q}} \tilde{\boldsymbol{x}}_\delta + \boldsymbol{u}^{\mathrm{T}} \boldsymbol{R} \boldsymbol{u}\right) dt < \gamma, \qquad (13)$$

where $\tilde{\boldsymbol{x}}_\delta := \left[\int_0^\infty (q_3^{\mathrm{ref}} - q_3)\,dt \ \int_0^\infty (q_4^{\mathrm{ref}} - q_4)\,dt \ \hat{\boldsymbol{x}}_\delta^{\mathrm{T}}\right]^{\mathrm{T}}$, $\tilde{\boldsymbol{Q}} = \tilde{\boldsymbol{Q}}_h^{\mathrm{T}} \tilde{\boldsymbol{Q}}_h \succeq \boldsymbol{0}, \boldsymbol{R} \succ \boldsymbol{0}, \boldsymbol{x}_0 := \boldsymbol{x}_e(0)$. The matrices $\boldsymbol{Q}$ and $\boldsymbol{R}$ are weighting matrices. A optimal controller that the initial-value response is improved is designed by minimizing γ under (13).

3.2 Design Condition

In this subsection, design conditions of the LPV model (10) are given by parameter-dependent linear matrix inequalities (PDLMIs). Let Ω_α, Ω_d, and Π be the parameter set of the scheduling parameters $\boldsymbol{\alpha}$, its derivatives $\dot{\boldsymbol{\alpha}}$, and initial-values $\boldsymbol{\alpha}_0 := \boldsymbol{\alpha}(0)$, respectively. If the motion range and the region of given initial-values are assumed such as $|q_i| \leq \bar{q}_i$ and $|q_{i0}| \leq \bar{q}_{i0}$, then parameter regions are defined as $|\alpha_i| \leq \sin \bar{q}_i$ and $|\alpha_{i0}| \leq \sin \bar{q}_{i0}$, respectively. The regions of the derivatives $\dot{\boldsymbol{\alpha}}$ is chosen as $|\dot{\alpha}_i| \leq \delta_i$. Note that the set Π satisfies $\Pi \subset \Omega_\alpha$. Those sets Ω_α, Ω_d, and Π are defined as follows:

$$\Omega_\alpha = \{\boldsymbol{\alpha} \in \mathbb{R} : \ g_j(\boldsymbol{\alpha}) \geq 0 \ (j = 1, \ 2)\}, \qquad (14)$$

$$\Omega_d = \{\dot{\boldsymbol{\alpha}} \in \mathbb{R} : \ g_j(\dot{\boldsymbol{\alpha}}) \geq 0 \ (j = 3, \cdots, 6)\}, \qquad (15)$$

$$\Pi = \{\boldsymbol{\alpha}_0 \in \mathbb{R} : \ g_j(\boldsymbol{\alpha}_0) \geq 0 \ (j = 7, \ 8)\}. \qquad (16)$$

In order to design the GS controller minimized γ under (13), sufficient conditions for the redundant descriptor system (10) are introduced as follows:

Proposition 3.1 : *If there exist polynomial matrices $\boldsymbol{X}_{11}(\boldsymbol{\alpha})$ and $\boldsymbol{Y}_1(\boldsymbol{\alpha})$ satisfying the following PDLMIs, the redundant descriptor system is stabilized by the state feedback $\boldsymbol{u} = \boldsymbol{Y}_1(\boldsymbol{\alpha}) \boldsymbol{X}_{11}^{-1}(\boldsymbol{\alpha}) \tilde{\boldsymbol{x}}_e$.*

minimized γ subject to;

$$\boldsymbol{F}_1(\boldsymbol{\xi}, \ \boldsymbol{\alpha}) := \boldsymbol{X}_{11}(\boldsymbol{\alpha}) \succ \boldsymbol{0} \ (\forall \boldsymbol{\alpha} \in \Omega_\alpha), \qquad (17)$$

$$\boldsymbol{F}_2(\boldsymbol{\xi}, \ \boldsymbol{\alpha}) :=$$

$$\begin{bmatrix} -\left(\mathrm{He}\left[\boldsymbol{\Phi}(\boldsymbol{\alpha})\right] - \hat{\boldsymbol{E}}_{\delta e} \dot{\boldsymbol{X}}(\boldsymbol{\alpha})\right) & * & * \\ \hat{\boldsymbol{Q}}_h \boldsymbol{X}(\boldsymbol{\alpha}) & \boldsymbol{I}_{13\times13} & * \\ \boldsymbol{R} \boldsymbol{Y}(\boldsymbol{\alpha}) & \boldsymbol{0}_{2\times13} & \boldsymbol{R} \end{bmatrix} \succ \boldsymbol{0}$$

$$(\forall (\boldsymbol{\alpha}, \ \dot{\boldsymbol{\alpha}}) \in \Omega_\alpha \times \Omega_d), \qquad (18)$$

$$\boldsymbol{F}_3(\boldsymbol{\xi}, \ \boldsymbol{\alpha}) := \begin{bmatrix} \gamma \boldsymbol{I}_{7\times7} & * \\ \boldsymbol{I}_{7\times7} & \boldsymbol{X}_{11}(\boldsymbol{\alpha}_0) \end{bmatrix} \succ \boldsymbol{0} \ (\forall \boldsymbol{\alpha}_0 \in \Pi), (19)$$

$$\boldsymbol{X}(\boldsymbol{\alpha}) := \begin{bmatrix} \boldsymbol{X}_{11}(\boldsymbol{\alpha}) & \boldsymbol{0}_{7\times6} \\ \boldsymbol{X}_{21}(\boldsymbol{\alpha}) & \boldsymbol{X}_{22}(\boldsymbol{\alpha}) \end{bmatrix},$$

$$\boldsymbol{Y}(\boldsymbol{\alpha}) := \begin{bmatrix} \boldsymbol{Y}_1(\boldsymbol{\alpha}) & \boldsymbol{0}_{2\times6} \end{bmatrix},$$

$$\boldsymbol{\Phi}(\boldsymbol{\alpha}) := \hat{\boldsymbol{A}}_{\delta e}(\boldsymbol{\alpha}) \boldsymbol{X}(\boldsymbol{\alpha}) + \hat{\boldsymbol{B}}_{\delta e}(\boldsymbol{\alpha}) \boldsymbol{Y}(\boldsymbol{\alpha}).$$

Then, the cost function J is less than γ.

Note that $\boldsymbol{\xi}$ is the vector of the decision variables $\boldsymbol{X}_{(i)}$, $\boldsymbol{Y}_{(i)}$, and γ. Let second-order polynomial matrices be the matrices $\boldsymbol{X}(\boldsymbol{\alpha})$ and $\boldsymbol{Y}(\boldsymbol{\alpha})$.

3.3 SOS Formulation

In this subsection, the design conditions as PDLMIs (17)-(19) in subsec. 3.2 are relaxed to sum of squares (SOS) conditions. Based on the results in [3], the PDLMIs are formulated to SOS conditions as follows:

Lemma 3.1 : *If there exist polynomial matrices $\boldsymbol{X}_{11}(\boldsymbol{\alpha})$ and $\boldsymbol{Y}_1(\boldsymbol{\alpha})$, and matrices SOS polynomials $\boldsymbol{S}_{10}$, $\boldsymbol{S}_{20}$, $\boldsymbol{S}_{30}$, $\boldsymbol{S}_{1j}$, $\boldsymbol{S}_{2k}$, and $\boldsymbol{S}_{3l}$ satisfying the following conditions (20)-(22), the redundant descriptor system is stabilized by the state feedback $\boldsymbol{u} = \boldsymbol{Y}_1(\boldsymbol{\alpha}) \boldsymbol{X}_{11}^{-1}(\boldsymbol{\alpha}) \tilde{\boldsymbol{x}}_e$.*

minimized γ subject to;

$$\boldsymbol{F}_1(\boldsymbol{\xi}, \ \boldsymbol{\alpha}) - \epsilon \boldsymbol{I}_{7\times7} - \sum_{j=1}^2 g_j(\boldsymbol{\alpha}) \boldsymbol{S}_{1j}(\boldsymbol{\alpha}) = \boldsymbol{S}_{10}(\boldsymbol{\alpha}), \ (20)$$

$$\boldsymbol{F}_2(\boldsymbol{\xi}, \ \boldsymbol{\alpha}) - \epsilon \boldsymbol{I}_{28\times28} \qquad (21)$$

$$-\begin{bmatrix} \left(\begin{array}{c} \sum_{k=1}^2 g_k(\boldsymbol{\alpha}) \boldsymbol{S}_{2k}(\boldsymbol{\alpha}) \\ + \sum_{k=3}^6 g_k(\dot{\boldsymbol{\alpha}}) \boldsymbol{S}_{2k}(\boldsymbol{\alpha}) \end{array}\right) & * \\ \boldsymbol{0}_{15\times13} & \boldsymbol{0}_{15\times15} \end{bmatrix} = \boldsymbol{S}_{20}(\boldsymbol{\alpha}),$$

$$\boldsymbol{F}_3(\boldsymbol{\xi}, \ \boldsymbol{\alpha}) - \epsilon \boldsymbol{I}_{14\times14}$$

$$-\begin{bmatrix} \boldsymbol{0}_{7\times7} & * \\ \boldsymbol{0}_{7\times7} & \sum_{l=7}^8 g_l(\boldsymbol{\alpha}_0) \boldsymbol{S}_{3l}(\boldsymbol{\alpha}_0) \end{bmatrix} = \boldsymbol{S}_{30}(\boldsymbol{\alpha}_0). \quad (22)$$

Then, the cost function J is less than γ.

4 Simulation

In this section, the effectiveness of the GS controller designed by the proposed approximation method (5) and (6) is illustrated by simulations. Here, an ordinary approximation method is defined as follows:

$$\begin{cases} \sin q_2 \simeq 0.9728 q_2 \\ \cos q_2 \simeq 1 - 0.4919 q_2^2 \end{cases}, \qquad (23)$$

$$\begin{cases} \sin q_3 \simeq 0.9945 q_3 - 0.1514 q_3^3 \\ \cos q_3 \simeq 1 - 0.4512 q_3^2 \end{cases}. \qquad (24)$$

Those trigonometric functions in (23) and (24) are approximated not the first-order but a high-order Taylor series expansion depending on q_i. Furthermore, in the same way as subsec. 2.3, the coefficients are optimized by using the method of least-squares to conduct more accurate approximation under the range (1) and (2), respectively. Let the proposed controller and the ordinary controller be the GS controllers designed by the proposed approximation method (5) and (6), and the ordinary approximation method (23) and (24). The proposed controller is compared with the ordinary controller designed by the simulations. The ordinary controller is designed by choosing the scheduling parameters $\boldsymbol{\rho} := [q_2 \ q_3]^{\mathrm{T}}$ based on matrix sum of squares (SOS) polynomials. Here, the following necessary conditions for the simulations are given in the controller design. Assume that the rotational speed of Rotor1 is constant value $\dot{q}_1 = 40$ [rad/sec]. The range of the angles q_2 and q_3, and its derivatives are assumed as follows:

$$|q_2| \leq \frac{\pi}{6}, \ |q_3| \leq \frac{5\pi}{12}, \ |\dot{q}_2| \leq 1.0, \ |\dot{q}_3| \leq 1.5. \quad (25)$$

The range of given initial-values are chosen as follows:

$$|q_{20}| \leq \frac{25\pi}{180}, \ |q_{30}| \leq \frac{5\pi}{12}. \quad (26)$$

Those GS controllers are designed by solving sufficient conditions in the lemma 3.1 under the necessary conditions (25) and (26). Thus, the upper bound value γ of each cost function are minimized. Those results are shown in Table 1. As can be seen in Table 1, the upper

Table 1 Upper bound value

proposed controller	$\gamma = 22.95$
ordinary controller	$\gamma = 27.97$

bound value produced by proposed controller is 17.95% lower than the upper bound produced by the ordinary controller.

By the results in [4], effect of the friction disturbance can't be ignored. Simulations which include effect of the friction disturbance are carried out. Let F_n ($n = 1, \cdots, 4$) be the friction disturbance for Rotor1, Gimbal2, Gimbal3, and Gimbal4, respectively. Let $f_{\mathrm{c},n}$ and $f_{\mathrm{v},n}$ be the coefficients of coulomb friction and viscous friction. The friction disturbance F_n is defined as follows:

$$F_n = f_{\mathrm{c},n} \arctan(\dot{q}_n \times 10^3) + f_{\mathrm{v},n}\dot{q}_n. \quad (27)$$

The simulations results are shown in Fig. 3 and 4 when the step reference $q_3^{\mathrm{ref}} = 1.0$ [rad] and $q_4^{\mathrm{ref}} = 1.0$ [rad] are given for the angles q_3 and q_4, respectively. The solid
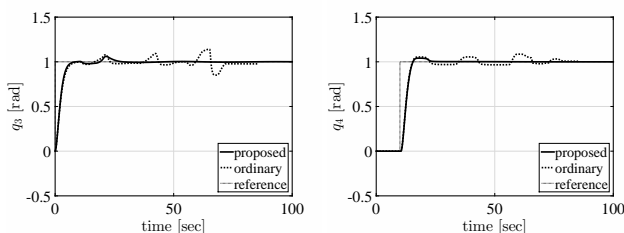
Figure 3 Responses of q_3 Figure 4 Responses of q_4

line and the dashed line show the responses of q_3 and q_4 by the proposed controller and the ordinary controller, respectively. The thin dotted line show the reference. As can be seen in Fig. 3 and 4, the responses of q_3 and q_4 by the proposed controller are improved. As a results of the simulations, the effect of the friction disturbance is reduced by using the proposed method.

5　Experiment

Experiments are carried out under the same situation indicated in sec. 4. The experimental results by the proposed controller are shown in Fig. 5 and 6. The
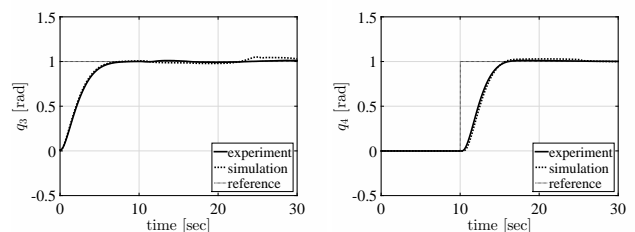
Figure 5 Responses of q_3 Figure 6 Responses of q_4

solid line and the dashed line show the responses of q_3 and q_4 by the simulation result and the experimental result, respectively. As can be seen in Fig. 5 and 6, the responses by proposed controller are stable, and follow the references without error. The reliability of the proposed controller is verified by the experimental results because the responses of the experiments are similar to the responses of the simulations.

6　Conclusion

This paper presents the GS controller design based on sum of squares (SOS) to solve nonlinear dynamics of the VSCMG. The highly accurate linear parameter varying (LPV) model is derived by using the proposed approximation. Design conditions are described by using PDLMIs to design the GS controller. The PDLMIs are relaxed to the sufficient conditions based on matrix SOS polynomials. Finally, the effectiveness of the proposed GS controller is shown by simulations and experiments comparing with the ordinary controller.

References

[1] H. Abbas, A. Ali, S. M. Hashemi and H. Werner: LPV Gain-Scheduled Control of a Control Moment Gyroscope. American Control Conference, pp. 6841-6846, 2013.

[2] H. Ichihara and M. Kawata: Gain Scheduling Control of an Arm-Driven Inverted Pendulum Based on Sum of Squares: Comparison with a SDRE Method. Proc. 18th World Congress, International Federation of Automatic Control, pp. 9613-9617, 2011.

[3] H. Ichihara and M. Kawata: Attitude Control of Acrobot by Gain Scheduling Control Based on Sum of Squares. American Control Conference, pp. 6636-6643, 2010.

[4] S. Washizu, C. Murai, I. Takami, and G. Chen: Nonlinear control for first-order nonholonomic system with hardware restriction and disturbance. Proceedings of 10th Asian Control Conference, PaperID 1570082557 (TS2.4-6-2), 2015.